Microelectronics Reliability 54 (2014) 629–632

Contents lists available at ScienceDirect

Microelectronics Reliability

journal homepage: www.elsevier.com/locate/microrel

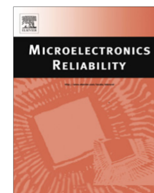

Effect of polyimide baking on bump resistance in flip-chip solder joints

Hsi-Kuei Cheng [a], Shien-Ping Feng [b], Yi-Jen Lai [c], Kuo-Chio Liu [c], Ying-Lang Wang [d,*], Tzeng-Feng Liu [a,*], Chih-Ming Chen [e,*]

[a] Department of Materials Science and Engineering, National Chiao Tung University, Hsinchu 300, Taiwan
[b] Department of Mechanical Engineering, The University of Hong Kong, Pokfulam, Hong Kong
[c] Backend Operations Division, Taiwan Semiconductor Manufacturing Company (TSMC), Ltd., Taiwan
[d] Institute of Lighting and Energy Photonics, National Chiao Tung University, Hsinchu 300, Taiwan
[e] Department of Chemical Engineering, National Chung Hsing University, Taichung 402, Taiwan

A R T I C L E I N F O

Article history:
Received 12 December 2012
Received in revised form 12 November 2013
Accepted 12 November 2013
Available online 2 December 2013

A B S T R A C T

The effect of polyimide (PI) thermal process on the bump resistance of flip-chip solder joint is investigated for 28 nm technology device with aggressive extreme low-k (ELK) dielectric film scheme and lead-free solder. Kelvin structure is designed in the bump array to measure the resistance of single solder bump. An additional low-temperature pre-baking before standard PI curing increases the bump resistance from 9.3 mΩ to 225 mΩ. The bump resistance increment is well explained by a PI outgassing model established based on the results of Gas Chromatography–Mass Spectrophotometer (GC–MS) analysis. The PI outgassing substances re-deposit on the Al bump pad, increasing the resistance of interface between under-bump metallurgy (UBM) and underneath Al pad. The resistance of interface is twenty-times higher than pure solder bump, which dominates the measured value of bump resistance. Low-temperature plasma etching prior to UBM deposition is proposed to retard the PI outgassing, and it effectively reduces the bump resistance from 225 mΩ to 10.8 mΩ.

© 2013 Published by Elsevier Ltd.

1. Introduction

Flip-chip package is the most important assembly method over the last decade especially for advanced fine-pitch devices [1,2]. Large number of tiny solder bumps are fabricated into an area array on a chip, where the bump plays an important role to connect the input/output (I/O) electronic signal between the chip and a package substrate. The diameter of the solder bumps is 100 m or less, and it continues to shrink for the purpose of small size and light weight. Typically, the resistance of a solder bump is estimated to be the order of few milli-ohms, whereas the resistance of the metallization trace ranges from few hundreds to few thousands of milli-ohms, depending on its dimension [3]. In general, the bump resistance is quite small compared with the resistance of the metallization traces. However, if the bump resistance is rose to few hundreds of milli-ohms, it will affect the transmission speed due to RC time delay.

Bump resistance measurement is a non-destructive detection which is usually used to monitor the tiny defect formation or microstructure changes in the solder bumps, especially for the investigations of bump reliability issues such as electromigration (EM) and temperature cycle (TC). Many literatures discussed the bump fatigue behavior during the reliability tests. The formation of voids and cracks in the solder bump induced bump resistance changes [4–7]. The Kelvin structure is designed in the ball grid array to measure the bump resistance and monitor the failure of EM and TC tests in flip-chip package. The bump resistance is increased gradually with increasing the stress time and finally opens while the solder bumps fail.

In this paper, we investigated the bump resistance changes with a polyimide (PI) layer covered on the chip surface. The purpose of PI layer is to release the thermal stress of solder bump and underneath extreme low-k (ELK) dielectric film during TC test. Typically, the PI film undergoes a curing process after photo development. An additional low-temperature pre-baking prior to curing was employed because it effectively enlarged the window of chip–package interaction (CPI) of flip-chip package especially for lead-free (LF) SnAg bumps. However, the pre-baking step caused a significant increment of the bump resistance. A mechanism of PI outgassing was proposed to explain the bump resistance increment based on the results of Gas Chromatography–Mass Spectrophotometer (GC–MS) analysis and an experiment of PI removal thickness on the bump resistance. This study provided a deeper understanding of the bump resistance change for LF flip-chip bump, and the results implied the bump resistance was a good indicator to monitor tiny abnormality of Fab PI process and bumping under-bump metallurgy (UBM) sputter process.

* Corresponding authors. Tel.: +886 6 3032535 (Y.L. Wang), tel: +886 3 5712121 31288 (T.F. Liu), tel.: +886 4 22859458 (C.M. Chen).
E-mail addresses: ylwang@tsmc.com (Y.-L. Wang), tfliu@cc.nctu.edu.tw (T.-F. Liu), chencm@nchu.edu.tw (C.-M. Chen).

0026-2714/$ - see front matter © 2013 Published by Elsevier Ltd.
http://dx.doi.org/10.1016/j.microrel.2013.11.006

2. Experimental procedures

The test vehicle employed in the bump resistance experiment was a 10 mm × 9 mm die that covered a HD4104 PI film on the top of chip. Photo development was performed on the PI film to form a circular opening on designed Al pad for subsequent UBM deposition. Prior to UBM deposition, two thermal processes of PI film were applied: mode-I was direct curing at 380 °C for about 2 min; mode-II was pre-baking the PI film at 200 °C for about 15 min before curing at 380 °C. After the PI thermal process, argon plasma etching at 250 °C for about 1 min was employed for surface cleaning. GC–MS was used to analyze the outgassing characteristics of the PI films thermally treated by two different modes mentioned above. It is a method that combines the features of gas–liquid chromatography and mass spectrometry to identify different substances within a test sample. Subsequently, Ti and Cu films were sequentially deposited on the Al pad using sputtering as the barrier and seed layers, respectively. Electroplating Ni UBM and LF SnAg (Ag = 1.8%) solder bump were made as the connection between the chip and a package substrate.

The Kelvin structure was designed in the bump array to monitor the resistance of single solder bump. A schematic drawing of the solder bump and Kelvin structure is shown in Fig. 1. The three solder bumps were connected by one Al metal line. A current (I_{12}) was forced through contact pin 1 to pin 2, and the voltage difference (ΔV_{34}) between contact pins 3 and 4 was detected. The resistance of single bump can be calculated as $\Delta V_{34}/I_{12}$.

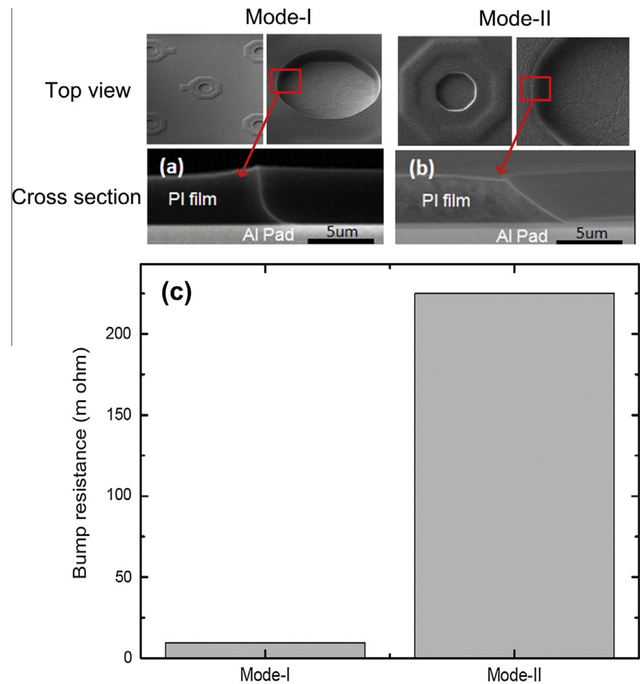

Fig. 2. Cross-sectional SEM images of PI opening for (a) mode-I and (b) mode-II. (c) Bump resistance measurement values of two different modes of PI thermal process.

3. Results and discussion

Fig. 2(a) and (b) shows the cross-sectional scanning electron microscopy (SEM) images of PI opening in mode-I and mode-II samples, respectively. It was found that the PI film shrunk slightly on the top of the opening as seen in Fig. 2(b) for mode-II sample, resulting in an increase of diameter at the top opening. Based on top-view observation, the diameter of the PI opening were comparable at the bottoms for both mode-I and mode-II samples (~30 m), but the top of the opening of mode-II sample was larger than mode-I by about 4 m in the diameter because the additional pre-baking resulted in slight PI film shrinkage. Considering the reliability issue of LF SnAg solder bump in advanced flip-chip package, the PI profile at the opening side is preferred to rounding shape as mode-II shown in Fig. 2(b). This is because a rounding shape of the PI opening side caused by an additional pre-baking at 200 °C can enlarge CPI window. The additional pre-baking employed in mode-II thermal process can also remove the moisture in the PI film. However, a side effect was found according to the results of bump resistance analysis. As the same scheme for flip-chip bump, the bump resistance of mode-II sample was rose twenty-time higher than that of mode-I one as shown in Fig. 2(c). The twenty-time increment in bump resistance should not be caused by the profile change of PI opening because the contribution of profile change is only the order of few milli-ohms. On the other hand, if the profile change of PI opening indeed affects bump resistance, the bump resistance should reduce for mode-II sample because of a larger area of the opening. Therefore, it implied that some other issue instead of the opening profile change was responsible for the resistance change and this issue should closely relate to the additional PI pre-baking at 200 °C employed in mode-II thermal process.

In addition to profile change of PI opening, pre-baking of the PI film at 200 °C for a relatively longer time (15 min) might also cause prominent degassing of some photosensitive and polymer compounds out of the PI film. To analyze the degassing phenomenon, the sample pre-baked at 200 °C was examined using GC–MS and the result was shown in Fig. 3(a). It was found that H_2O, CO, CO_2, photo-sensitive and monomer were diffused out of the PI film after pre-baking at 200 °C (mode-II). The PI film after 380 °C curing (mode-I) was also examined using GC–MS and only few H_2O, CO and CO_2 were released because of a shorter curing time (2 min) as seen in Fig. 3(b). Based on the above results of GC–MS analysis, a model of PI outgassing was proposed to explain the mechanism of the resistance difference between mode-I and mode-II PI films. Fig. 4(a)–(c) represent the PI status at each step in mode-I thermal process. After photo development, unstable substances, say, outgassing source like solvent and partial-linked PI, were uniformly distributed in the PI film as the solid spots in Fig. 4(a). The uniform distribution of unstable substances could be approximately

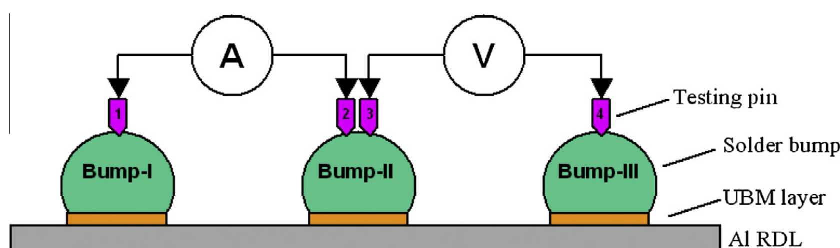

Fig. 1. Schematic diagram of solder bump and Kelvin structure.

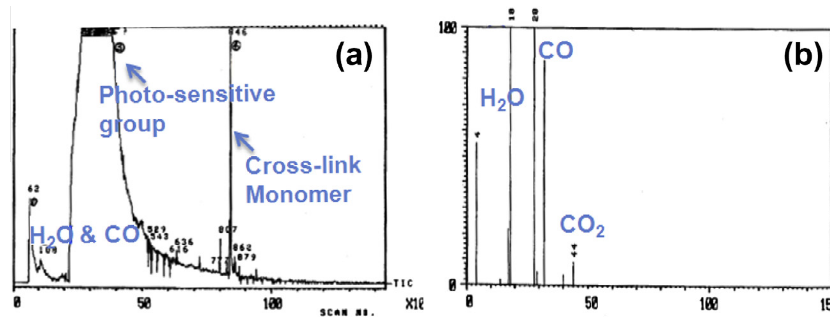

Fig. 3. GC–MS analysis results of (a) the PI film after pre-baking at 200 °C in the mode-II thermal process and (b) the PI film after curing at 380 °C in the mode-I thermal process.

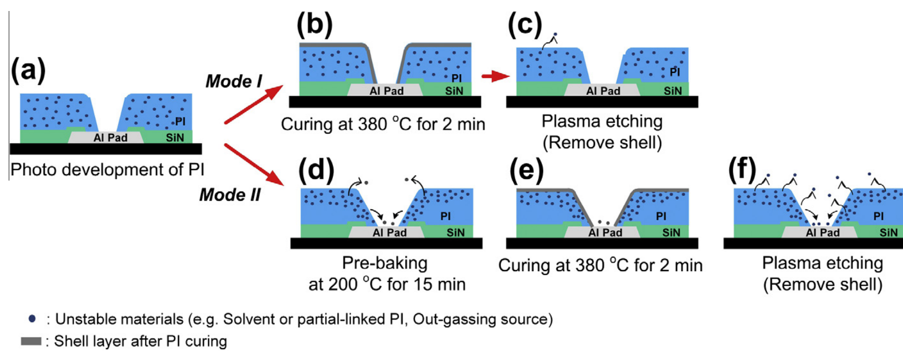

Fig. 4. Illustration of the mechanism of PI outgassing model: (a) photo development, (b) post PI curing at 380 °C, (c) during plasma etching of mode-I PI film, (d) the PI low-temperature pre-baking at 200 °C, (e) post PI curing at 380 °C, and (f) during plasma etching of mode-II PI film.

retained in the PI film after 380 °C curing, as shown in Fig. 4(b), because the curing time was too short (2 min) to disturb them. During curing, the PI film also quickly formed a hard shell on the surface. The hard shell was suggested to be able to lock most of the unstable substances within the PI film, so the outgassing degree was negligible. That was the reason why only few H_2O, CO and CO_2 were detected as mentioned above. After curing, the hard shell needed to be removed by argon plasma etching (250 °C for 1 min) in order for subsequent UBM deposition. Because the wafer temperature in the plasma chamber was about 250 °C, small amount of outgassing occurred mainly from the surface of the PI film as shown in Fig. 4(c).

By contrast, for mode-II PI thermal process, an additional pre-baking at 200 °C took a relatively longer time (15 min) which caused prominent degassing as mentioned above. More photosensitive and polymer compounds would also be trapped (segregated) at the PI surface as shown in Fig. 4(d). As a result, the unstable substances trapped (segregated) at the PI surface could easily diffuse out during the plasma etching process at 250 °C. Some released compounds re-deposited on the Al pad as shown in Fig. 4(f) which acted as tiny defects at the interface between Al pad and subsequently-deposited UBM layer, leading to an increment of the bump resistance. Energy-dispersive X-ray spectrometer (EDX) examination of the Al surface was performed to validate the deposition of released compounds and the results were shown in Fig. 5. It was found that the Al surface of mode-I displayed negligible signals of carbon and oxygen, but that of mode-II showed stronger signal intensity of carbon and oxygen, indicating that higher amount of released compounds indeed deposited on the Al surface of mode-II.

As suggested in Fig. 4(d), more unstable substances were trapped (segregated) at the PI surface after the pre-baking step in the mode-II thermal process. It implied that if the surface portion of the PI film was removed, the unstable substances at the PI surface could also be removed simultaneously. This could reduce the amount of outgassing from the PI surface during the subsequent curing and plasma etching steps. To further verify the outgassing model, an experiment of PI removal thickness on the bump resistance was performed. An additional step was added to remove the PI surface by O_2 plasma etching (100 °C for 30 s) after the pre-baking step while the other steps were unchanged in the

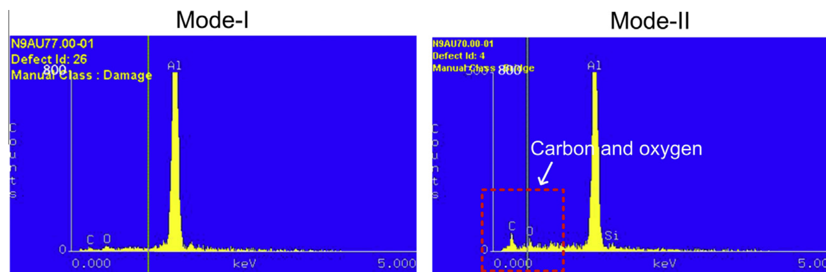

Fig. 5. EDX examination of the Al surfaces for mode-I and mode-II thermal processes.

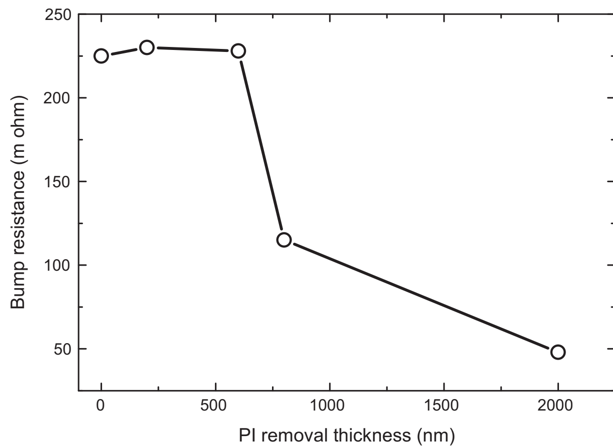

Fig. 6. The bump resistance trend of mode-II PI film with the PI removal thickness by O_2 plasma etching.

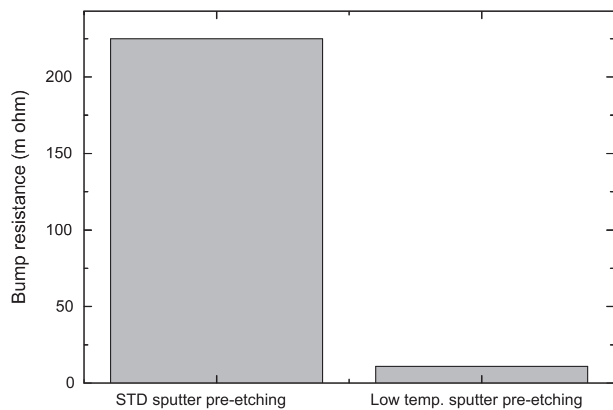

Fig. 7. Bump resistances of mode-II PI with two different temperatures for argon plasma etching before UBM deposition.

mode-II thermal process. From Fig. 6, the bump resistance kept high for less PI removal thickness but rapidly reduced when the removal thickness of the PI film exceeded 6 kÅ. The result was in good agreement with our expectation. Because most of the unstable compounds were trapped (segregated) at the PI surface, the effects of outgassing and re-deposition of unstable compounds on the Al surface kept worse if only little PI thickness was removed. However, once the PI removal thickness over a critical value (~6 kÅ), the bump resistance was reduced significantly due to only less outgassing source remained in the deeper PI film.

The effect of temperature for argon plasma etching on the bump resistance was also investigated. Fig. 7 shows the bump resistances for two different etching temperatures. The left was the bump resistance (225 m) for the mode-II thermal process in which the wafer temperature in the plasma etching chamber was 250 °C. The right showed that the bump resistance was significantly reduced to 10.8 m when the wafer temperature in the plasma etching chamber was cooled down to 150 °C by employing water cooling kits. The value was comparable to that of a pure solder bump. It was suggested that low-temperature plasma etching retarded the outgassing of the PI film and re-deposition of unstable compounds on the joint interface, and the bump resistance did not increase accordingly.

4. Conclusions

The effect of an additional PI pre-baking process on the bump resistance of flip-chip solder bumps was investigated. A significant increment of bump resistance due to additional low-temperature pre-baking was found. Based on the GC–MS analysis results, the resistance change was reasonably explained by a PI outgassing model. The model was verified by an experiment of PI removal thickness on the bump resistance. The additional pre-baking step resulted in more photosensitive and polymer compounds being trapped (segregated) at the PI surface. The unstable compounds diffused out during the plasma etching process that was performed at 250 °C before UBM deposition. As a result, some unstable compounds re-deposited on the Al pad as tiny defects, leading to high resistance at the interface between Al pad and UBM layer. To avoid significant increase of the bump resistance, we proposed a low-temperature plasma etching step at 150 °C prior to UBM deposition to reduce the PI outgassing by employing water cooling kits. The bump resistance of mode-II PI thermal process was significantly reduced from 225 m to 10.8 m which was comparable to the estimated performance of pure solder bump.

Acknowledgements

The authors thank Taiwan Semiconductor Manufacturing Company and Department of Materials Science and Engineering, National Chiao Tung University, Hsinchu, Taiwan, for technical support.

References

[1] International technology roadmap for semiconductors. San Jose, CA: Semiconductor Industry Association; 2003; p. 4–9.
[2] Tu KN, Zeng K. Mater Sci Eng R 2001;R34:1.
[3] Shao TL, Chiu SH, Chen C, Yao DJ, Hsu CY. J Electron Mater 2004;33:1350.
[4] Liu DS, Ni CY. Microelectron Eng 2002;63:363.
[5] Tu KN. J Appl Phys 2003;94:5451.
[6] Gee S, Nguyen N, Huang J, Tu KN. In: Proceedings of international wafer-level packaging conference (IWLPC). San Jose, CA: Surface Mount Technology Association; 2005, p. 159–67.
[7] Su P, Ding M, Uehling T, Wontor D, Ho PS. In: Proc Electron Comp Technol Conf. Piscataway, NJ: IEEE; 2005. p. 1431–36.